ECOLOGY LETTERS

Ecology Letters, (2012) **15**: 1406–1414 doi: 10.1111/j.1461-0248.2012.01864.x

LETTER

Amazon forest carbon dynamics predicted by profiles of canopy leaf area and light environment

Scott C. Stark,[1*] Veronika Leitold,[1] Jin L. Wu,[1] Maria O. Hunter,[2] Carolina V. de Castilho,[3,14] Flávia R. C. Costa,[3] Sean M. McMahon,[4,5] Geoffrey G. Parker,[4] Mônica Takako Shimabukuro,[6] Michael A. Lefsky,[7] Michael Keller,[2,8,15] Luciana F. Alves,[1,9,10] Juliana Schietti,[3] Yosio Edemir Shimabukuro,[6] Diego O. Brandão,[3] Tara K. Woodcock,[1] Niro Higuchi,[11] Plinio B. de Camargo,[12] Raimundo C. de Oliveira[13] and Scott R. Saleska[1]

Abstract

Tropical forest structural variation across heterogeneous landscapes may control above-ground carbon dynamics. We tested the hypothesis that canopy structure (leaf area and light availability) – remotely estimated from LiDAR – control variation in above-ground coarse wood production (biomass growth). Using a statistical model, these factors predicted biomass growth across tree size classes in forest near Manaus, Brazil. The same statistical model, with no parameterisation change but driven by different observed canopy structure, predicted the higher productivity of a site 500 km east. Gap fraction and a metric of vegetation vertical extent and evenness also predicted biomass gains and losses for one-hectare plots. Despite significant site differences in canopy structure and carbon dynamics, the relation between biomass growth and light fell on a unifying curve. This supported our hypothesis, suggesting that knowledge of canopy structure can explain variation in biomass growth over tropical landscapes and improve understanding of ecosystem function.

Keywords

Biomass growth, carbon balance, gap fraction, leaf area profiles, remote sensing of canopy structure, LiDAR.

Ecology Letters (2012) **15**: 1406–1414

INTRODUCTION

A challenge in ecosystem science is to understand carbon dynamics in tropical forests, of which the Amazon is the largest region with the largest potential feedbacks to global climate change. Amazonian forests face an uncertain future: the Amazon is expected to warm and experience lower rainfall and an increased frequency of severe drought in the coming century (Cox *et al.* 2004; Malhi *et al.* 2008; Sitch *et al.* 2008). Evidence suggests that drought may have rapid widespread effects on carbon dynamics and canopy structure, particularly by increasing the mortality rate of large trees (Nepstad *et al.* 2007; Phillips *et al.* 2009). Although canopy environments may strongly mediate ecosystem carbon dynamics by influencing photosynthetic production and tree performance – including recruitment, growth and mortality – the exact nature of this mediation is not well known (Moorcroft 2006; Niinemets & Anten 2009).

Historically, investigation into tropical forest above-ground carbon dynamics has followed two distinct trajectories. First, scaling the biophysics of leaf photosynthetic production (via process models) to predict the influence of canopy environments on gross primary production (e.g. de Pury & Farquhar 1997). Second, linking forest demography (the growth, mortality and recruitment of individual trees or groups of trees, as acquired from permanent tree inventory plots) directly to above-ground ecosystem carbon dynamics (e.g. Lewis *et al.* 2004; Muller-Landau *et al.* 2006b). Contemporary research aims to unite leaf-scale biophysics and forest demographic processes to establish a mechanistic predictive framework to link environments with ecosystem carbon dynamics. The performance of trees across the forest size spectrum must be connected with the canopy environments that drive leaf biophysics (Kohyama 1993; Moorcroft *et al.* 2001; Muller-Landau *et al.* 2006b). Methods to measure three-dimensional variation in canopy structure and environments at sufficient spatial scales to link with tree performance, however, have been lacking.

Airborne small-footprint LiDAR is typically used to improve estimates of landscape-scale ecosystem carbon stocks (Chambers *et al.*

[1]*Department of Ecology and Evolutionary Biology, University of Arizona, Tucson, AZ, 85721, USA*
[2]*Complex Systems Research Center, University of New Hampshire, Durham, NH, 03824, USA*
[3]*Instituto Nacional de Pesquisas da Amazônia (INPA), Coordenação de Pesquisas em Ecologia, Manaus, AM, 69011-970, Brazil*
[4]*Smithsonian Environmental Research Center, Forest Ecology Group, P.O. Box 28, Edgewater, MD, 21037, USA*
[5]*Center for Tropical Forest Science, Smithsonian Tropical Research Institute, Apartado Postal 0843-03092, Panamá*
[6]*Brazilian Institute for Space Research (INPE), São José dos Campos, 12227-010, São Paulo, Brazil*
[7]*Natural Resource Ecology Laboratory, Colorado State University, Fort Collins, CO, 80523, USA*
[8]*International Institute of Tropical Forestry, USDA Forest Service, San Juan, 00926, Puerto Rico, USA*
[9]*Instituto de Botânica, Núcleo de Pesquisa em Ecologia, 01031-970, São Paulo, Brazil*
[10]*Institute of Arctic and Alpine Research (INSTAAR), University of Colorado, Boulder, CO, 80309, USA*
[11]*Coordenacão de Pesquisas em Silvicultura Tropical, Instituto Nacional de Pesquisas da Amazônia, Caixa Postal 478, Manaus, AM, 69011-907, Brazil*
[12]*Laboratório de Ecologia Isotópica, Centro de Energia Nuclear na Agricultura (CENA), Universidade de São Paulo, 13400-970 Piracicaba, São Paulo, Brazil*
[13]*Embrapa Amazônia Oriental, 68035-110 Santarém, Pará, Brazil*
[14]*Embrapa Roraima, 69301-970, Boa Vista, Roraima, Brazil*
[15]*Embrapa Monitoramento por Satélite, Avenida Soldado Passarinho, 303, Fazenda Chapadão, Campinas, São Paulo, Brazil*
**Correspondence: E-mail: scott.c.stark@gmail.com*

2007; Asner *et al.* 2010). We examine whether this technology can be applied to predict the components of above-ground carbon dynamics based on data on canopy structure. Our approach relates the above-ground coarse wood production (biomass growth) of trees in different *size groups* (size classes from particular forest inventory plots) with LiDAR-based estimates of light transmittance and absorption and leaf area density in different, associated, canopy strata. We formulate hypotheses that depend on the importance of light environments and how these environments are distributed over the forest size spectrum, and use our data to test these in comparison to alternative simpler hypotheses that do not account for the distribution of biomass over canopy environments.

The optimisation of leaf and individual tree production may help explain canopy structure and function (reviewed in Niinemets & Anten 2009). Under optimisation, we may expect consistent relationships between canopy environments and canopy production, in the face of variation in other characteristics such as maximum tree height (Hypothesis **H1a**). On the other hand, variation in canopy production could be related to other factors (Hypothesis H1b), potentially obscuring relationships between canopy environments and biomass growth. Plots or sites may differ in the heights (diameters) of the groups associated with particular crown environments – this could lead to different patterns of biomass growth if leaf function is more sensitive to height than environment (Cavaleri *et al.* 2010). Tree allocation towards wood production may slow as trees get larger (Herault *et al.* 2011; Coomes *et al.* 2012), while leaf area may differ between groups in similar environments because of differences in demographic history that lead to differences in the number of individuals in groups (Muller-Landau *et al.* 2006b). Finally, leaf ecophysiology could differ between plots and sites because of differences in functional composition or nutrient and water resources (Lambers *et al.* 2008).

If we find support for **H1a**, consistent relationships between canopy environments and biomass growth may help illuminate the environmental drivers of biomass growth and allow airborne LiDAR to assess landscape carbon dynamics, thus helping to resolve debates about whether the Amazon is a source or sink of atmospheric CO_2 today (Gloor *et al.* 2009). If we instead find support for **H1b**, other factors such as leaf functional characteristics or soil heterogeneity may be critically important covariates needed to link ecosystem biomass growth with canopy environments.

We also hypothesised that simpler indices may predict elements of above-ground carbon dynamics, but only insofar as these indices strongly reflect the integrated influence of canopy structure and environments on canopy function (**H2**). Particularly, we hypothesised that canopy gap fraction (fraction of canopy vegetation lower than a threshold height) and the canopy Shannon index (a combined measure of the extent and evenness of canopy area profiles) were two such indices.

MATERIALS AND METHODS

Study sites

Plots were from the Adolfo Ducke Reserve (Manaus, Amazonas, Brazil) and the Tapajós National Forest (Santarém, Pará, Brazil; 500 km east of Manaus), a site previously found to be out of demographic equilibrium, possibly due to past disturbance (Saleska *et al.* 2003; Vieira *et al.* 2004; Castilho *et al.* 2006; Pyle *et al.* 2008). Both sites are *terra firme* forest but differ in that the Tapajós has more pronounced dry season (5 mo. vs. 3 mo. with <100 mm rainfall mo^{-1}). Ducke and the nearby ZF2 site - also considered in gap fraction analysis - sample more soil conditions ranging from sandy valleys to adjacent clay-rich plateaus ~50–100 m higher (da Silva *et al.* 2002; Vieira *et al.* 2004; Castilho *et al.* 2006; Pyle *et al.* 2008). For additional detail see Appendix S1.

Diameter surveys and biomass dynamics

Tree diameter survey plots were long-term – predating this study – and followed standard tropical forest methodologies for measurements (Appendix S1; da Silva *et al.* 2002; Castilho *et al.* 2006). Plots at both sites were constant in elevation along 250 m elongated central axes and were variable in area for trees of different size classes, sampling 1 hectare (ha) and 1.25 ha for trees over 30 cm diameter at breast height (DBH), or over 35 cm DBH, in the Ducke and the Tapajós sites respectively. The minimum tree diameter considered in both sites was 10 cm DBH, but Ducke included individuals between 1 and 10 cm DBH. All analyses were standardised to the one-hectare scale. Ducke one-hectare scale plots ($N = 22$) were separated by 1 km in a grid design (Fig. S1). We subdivided four large plots in the Tapajós – associated with a gas exchange eddy flux tower – into 16 subplots (Fig. S2; total plots $N = 38$). We used the third-order polynomial biomass allometry for tropical wet forest presented in Chave *et al.* (2005) to estimate biomass (aboveground coarse wood carbon density, Mg C ha^{-1}) from (1) DBH measurements, (2) species, genera or community-average wood density values (Pyle *et al.* 2008; Chave *et al.* 2009) and (3) plot areas. In Appendix S1, we also present components of carbon dynamics estimated from a recent, alternate, biomass allometry that incorporates region-specific height vs. diameter relationships (Feldpausch *et al.* 2012) for comparison with components estimated from the Chave *et al.* (2005) allometry; we found that the sign, R^2, and statistical significance of reported relationships were effectively unaltered by the choice of biomass allometry but that estimates from the Feldpausch *et al.* (2012) allometry were ≈20% lower. To reduce measurement error, we probabilistically filtered data to central 95% quantiles of annual diameter increment (cm yr^{-1}), replacing values outside of this range with individual-specific predictions from a multiple regression model on past and subsequent (when available) measurements. We chose single census intervals 4 years in length immediately leading up to or including the LiDAR acquisition in 2008 for biomass dynamics analysis (Ducke 2004–2008, Tapajós 2005–2009). We note that allometric biomass estimation, while the best approach available, entails significant uncertainty (Chave *et al.* 2004; Pyle *et al.* 2008; Feldpausch *et al.* 2012).

LiDAR data acquisition

All sites were over flown between the 7th and the 28th of June 2008 with a Leica Geosystems ALS70-II LiDAR (Heerbrugg, Switzerland). Ground LiDAR surveys were conducted at Ducke and the Tapajós in April and August of 2009, respectively, with a Riegl LD90-3100VHS-FLP system (Horn, Austria). Although the airborne LiDAR surveys generated a three-dimentional data set, ground LiDAR surveys generate a canopy profile map in the vertical and a single horizontal direction (Parker *et al.* 2004). We analysed airborne LiDAR data from central 10-m wide regions of forest plots.

Airborne LiDAR data were associated with forest plots based on differential GPS measurements and a distance-decay optimisation of the likelihood of canopy surface profile correlation between airborne and ground-based LiDAR (P-value < 0.001 in all plots; mean $R^2 = 0.5$ after smoothing ground-based estimates; Appendix S1). Maximum canopy height estimates corresponded to within a few meters.

Estimating canopy structure and light environments from LiDAR

We estimated leaf area profiles from the distribution of airborne LiDAR returns, adjusting for shadowing of canopy elements further from the sensor by the nearer elements using the MacArthur & Horn (1969) method. In a novel approach, we tested how well this adjustment worked by comparing with similar profiles, but derived from a ground-based LiDAR that viewed the forest from the opposite direction. Specifically, we derived leaf area estimates by (1) assuming an exponential reduction of LiDAR pulses by leaf area through successive 1-m thick (vertical dimension) canopy voxels with 10 m^3 volume – ~12,500 per plot – and (2) adjusting the exponential constant so that total leaf area (LAI) matches published values for LAI in the central Amazon (i.e. 5.71; Appendix S1). Airborne LiDAR-derived mean leaf area density profiles showed strong agreement with ground LiDAR-derived profiles in the Tapajós and Ducke, relative to the difference between sites (Fig. 1a and b), and with a destructive estimate of the Ducke vertical leaf area profile (McWilliam *et al.* 1993; Fig. 1a for Ducke). This test gave us confidence in the reliability of airborne LiDAR indices. Although LiDAR has been applied to estimate leaf area profiles, relatively few studies have validated these estimates (e.g. Harding *et al.* 2001; Parker *et al.* 2001; Tang *et al.* 2012).

The distribution of leaf area determines the distribution of light and the pattern of light absorption in the canopy (Parker *et al.* 2001; Todd *et al.* 2003; Lee *et al.* 2009; Richardson *et al.* 2009). Therefore, we also derived profiles of two indices of light environment to associate with plots and sites: the estimated fractional transmittance of light incident to the canopy, an index of relative light availability at a given point in the canopy (Fig. 1c), and the estimated light absorption within a given canopy layer (fraction of incident light; Fig. 1d). These light indices corresponded with light that passes through the canopy vertically and do not consider reflectance and scattering. The exponential reduction of LiDAR pulses used to estimate leaf area density is similar to that influencing photosynthetically active radiation (PAR) transmittance (Parker *et al.* 2001), however, the rate of LiDAR pulse reduction is expected to differ from that of PAR since LiDAR employs a different wavelength: near infrared (NIR). Therefore, we adjusted exponential light attenuation constants to create understory light conditions that agreed with empirical measurements. Absorption was calculated as the difference in light transmittance between the top and bottom of each voxel. Although light environments are mechanistically connected to the arrangement of leaf area, the leaf area density of a particular voxel does not directly influence the incoming light such that these variables are independent. Absorption may be influenced by covariation between leaf area density and light transmittance. Confidence intervals (95%) bracketing mean profiles of leaf area density and light indices were bootstrapped while controlling for horizontal spatial autocorrelation in leaf area from 1 to 12 m.

Predicting biomass growth of size groups with LiDAR-derived canopy indices

We tested whether canopy variables estimated from LiDAR predicted biomass growth across the tree size spectrum. We divided tree samples in one-hectare plots into size groups of trees defined by 10-cm wide DBH bins (e.g. trees 10–20 cm DBH form a size group). We associated the biomass growth of size groups with LiDAR-derived estimates of leaf area density and the transmittance

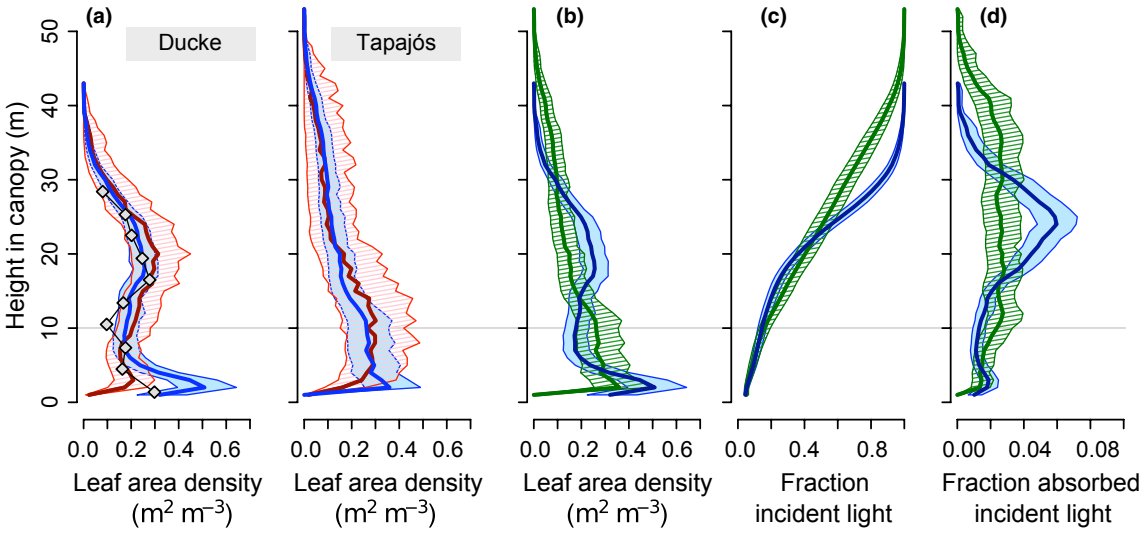

Figure 1 Panel *a*: validation analysis of LiDAR-derived estimates of leaf area density (m^2 m^{-3}) for both sites. We compared profiles estimated with ground-based LiDAR (*red*, *hashed*) and co-located airborne LiDAR (*blue*, *solid*). Means are heavy lines within the hashed (or solid) 95% CI envelopes. Gray diamonds show destructive leaf area measurements collected near Ducke by McWilliam *et al.* (1993). The next panels show site differences in airborne LiDAR-derived estimates of leaf area density (panel *b*), fractional transmittance of vertically incident light (panel *c*) and the absorption fraction of vertically incident light (panel *d*) between Ducke (*blue*, *solid*) and Tapajós (*green*, *hashed*) sites. Trees associated with heights lower than 10 m (thin-grey line) were not employed in site comparison analyses.

and absorption of incident light. Size groups were connected with canopy environments based on the expected position (height) of their crowns in the canopy, based on a power-law allometry relating diameter and crown height in tropical trees (Chave *et al.* 2005; Feldpausch *et al.* 2010). We based crown height expectations on an eastern Amazon-specific allometry generated from a large multi-site analysis [Feldpausch *et al.* 2010; Height in $m = 3.178\times$ (Diameter in cm) $^{0.5072}$]. Each size group corresponds with an expected region in the canopy – a horizontal stratum – with lower and upper bounds determined by the allometric height expectations for the smallest and largest tree diameters in the size group (e.g. 10–20 cm DBH corresponds with a canopy stratum extending from 10 to 15 m). Each one-hectare plot was subdivided into 23 horizontal strata containing up to 23 size groups (not all strata need be occupied by tree crowns, see Fig. 2; total $N = 351$). This approach does not consider variation in the height diameter allometry or in the depth of tree crowns.

Within vertical strata, we calculated spatial means of LiDAR-based estimates of leaf area density, light availability and light absorption to compare with size group biomass growth (Fig. 2). Taking spatial means reduces or eliminates the possibility that predictable variation in the vertical extent of canopy strata is statistically confounded by correlations with tree size groups. Spatial mean leaf area density is not a measure of the total leaf area associated with a size group. Instead, relative differences in size group total leaf area can be estimated by comparing total basal areas – basal area has been found to be directly proportional to leaf area (Shinozaki *et al.* 1964; Fownes & Harrington 1992; Enquist & Niklas 2002). Basal area specific biomass growth is likely, therefore, to be directly proportional to leaf area specific biomass growth.

To test the predictive skill of models of biomass growth based on LiDAR-estimated variables, we restricted the statistical analysis to plots from the Ducke reserve, but we applied this model predictively (i.e. with fit coefficients from Ducke) to all plots at both sites. We aggregated model predictions of size structure within sites (i.e. collecting size groups of the same size) and by summing size groups in each one-hectare plot, to compare with tree plot estimated biomass growth.

Gap fractions, canopy heights and the canopy Shannon index

To test the hypothesis that simple metrics of integrated forest structure and environmental variation derived from LiDAR can predict biomass growth, we calculated gap fraction and the canopy Shannon index and compared them against single canopy layer metrics like LAI. We generated digital canopy height models (CHMs) by fitting a surface through local minima (ground surface) and maxima (outer forest canopy surface) of LiDAR point cloud data, and taking the difference between these surfaces at a 1 m^2 resolution (Chen *et al.* 2007). Gap fraction is a fraction of forest area, where the canopy height is less than the threshold defined for a gap (Brokaw 1985) and may combine information on demographic and canopy structure and environments because gaps reflect a history of tree mortality and influence light environments and leaf area (Clark *et al.* 2008). We use a threshold height of 10 m for a gap, and also require that a gap occupy a contiguous area of at least 10 m^2. Work in progress suggests that this definition optimises the sensitivity of gap fraction to elements of forest dynamics. For larger areas within sites, we calculated gap fraction in a window encompassing all forest plots comprising the larger area. For individual 1 ha plots, gap fraction and canopy height were calculated from windows corresponding to GPS estimates of tree plot boundaries. The Shannon index quantifies information entropy (see Appendix S1) and in this case, applied to leaf area density profiles, it is a measure of canopy structural diversity, increasing with the vertical extent of the profile and with a more equal distribution of leaf area density across the profile. The canopy Shannon index is sensitive to the vertical dimension of canopy voxels (standardised to 1 m).

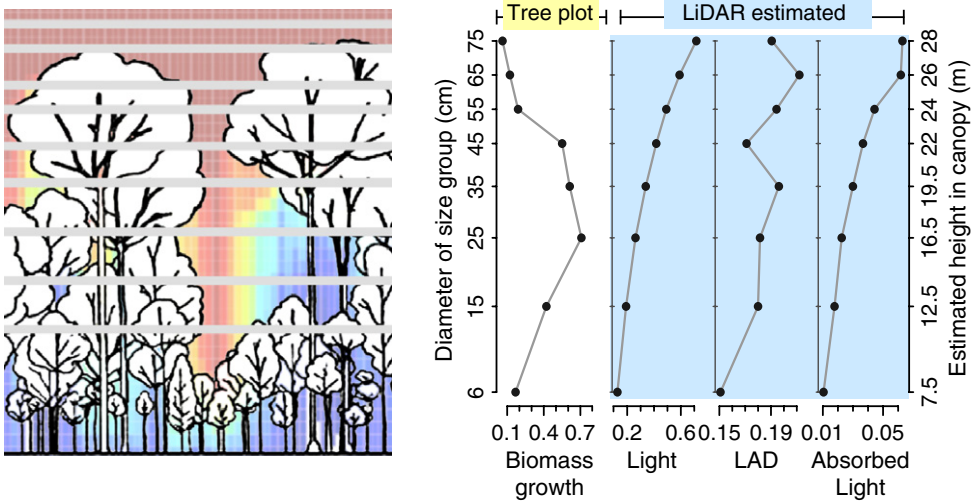

Figure 2 Size group data set: The total above-ground coarse wood production (biomass growth, Mg C ha^{-1} yr^{-1}) of trees in size groups were associated with LiDAR-based estimates of leaf area density, light availability and absorption in canopy strata. Trees in a forest plot (redrawn from Davis & Richards 1933) intersect maps of light transmittance (multi-colour underlay), and other LiDAR-estimated canopy variables. *Size groups were associated with particular strata – shown between grey horizontal bars – based on expected crown heights.* Crown height expectations were based on an empirical height-diameter allometry from the eastern Amazon (Feldpausch *et al.* 2010). Strata divisions corresponded to diameters at the boundaries of 10 cm-DBH size-classes. The figure panels on the right – showing the size group data set for one of 36 plots – are biomass growth and LiDAR-estimated mean leaf area density (LAD, m^2 m^{-3}), light transmittance (Light) and absorbed light (Absorbed Light, see also Fig. 1).

RESULTS

LiDAR-derived estimates of canopy structure and environment predicted variation in biomass growth – i.e. above-ground coarse wood production (Mg C ha^{-1} yr^{-1}) – over tree size groups, forest plots and sites. Furthermore, the relationship between estimated light transmittance and size group biomass growth was explained by a single curve common to both sites, supporting H1a and suggesting that the higher biomass growth of the eastern site results from more size groups in intermediate light environments.

Canopy leaf area structure and light environments

We found that the Tapajós forest is taller with more estimated leaf area in the sub-canopy than Ducke (Figs. 1b, S5 and S6), despite similar total Leaf Area Index values (LAI, leaf area summed vertically; 5.72 and 5.70 respectively). Profiles show a strong peak in estimated light absorption at about 25 m in Ducke, while in the Tapajós there is evidence of a large plateau in absorption extending from 12 m to 37 m (Fig. 1d). Average estimated light transmittance appears to decrease more rapidly in Ducke and attains a low level higher in the canopy than the Tapajós, despite the taller canopy of the Tapajós (Fig. 1c).

Predicting size group biomass growth from canopy structure and environment

We analysed how LiDAR-derived canopy indices were related to above-ground biomass dynamics, particularly biomass growth. Comparing sites, considering bootstrapped 95% confidence regions, size group biomass growth appeared consistently related to only one factor: mean light availability (Figs. 3 and S9). Although biomass growth declined with higher light, basal area specific biomass growth – a metric of leaf area specific wood production – was relatively constant over light environments and sites (Fig. 3). Basal area significantly declined with increasing light and was consistently related to biomass growth (Fig. S9d). Although the best linear model predicting basal area with light included a site level effect on the slope and intercept terms (R^2 = 0.70, *P*-value < 0.0001), differences between site relationships appeared modest. At 20% estimated transmission, Ducke was expected to have 28% more basal area than the Tapajós, but the difference was less than 1% at 90% of incident light. Site and plot-level variation in standing biomass were strongly predicted by LiDAR data (between 40 and 55% of variation), as has been found by other studies (Fig. S10).

Relating biomass growth with LiDAR-based metrics, we restricted analysis to the tree size classes common between sites (trees >10 cm DBH) and excluded data from an outlier plot (lowest biomass growth; Ducke *LO3.4500*). Substantial variation in leaf area density, light transmittance and light absorption remained after correlation with each other factor, suggesting that these factors could be included together in a multiple linear model (leaf area density vs. light: R^2 = 0.47, *P*-value < 0.0001; leaf area density vs. absorption: R^2 = 0.31, *P*-value < 0.0001; light vs. absorption: R^2 = 0.01, *P*-value = 0.07). A multiple linear model including all three factors was identified by AIC analysis as the best model explaining the biomass growth of size groups in Ducke plots (Ducke model: biomass growth = 0.554 + 1.119 × leaf area density −3.927 × light absorption −0.484 × light transmittance; Resid. SE = 0.15; R^2 = 0.66; 161 d.f.; *P*-value < 0.0001; additional results in Appendix S1). This

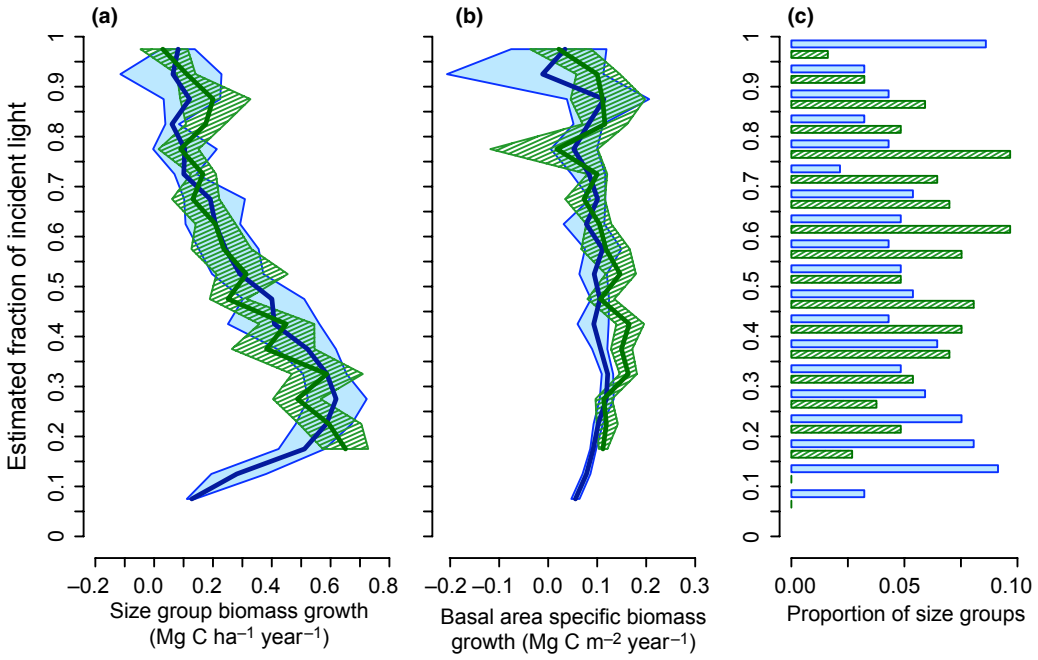

Figure 3 Relationships between biomass growth and basal area specific biomass growth in tree size groups and mean light transmittance (estimated with LiDAR) are consistent between Ducke (*blue*, *solid*) and Tapajós (*green*, *hashed*) sites (panels *a* and *b*). Hashed (or solid) regions show 95% confidence intervals based on resampling size groups falling within bins defined by similar light availability (20 bins). Extension into lower light transmittance was possible at the Ducke site, where individuals under 10 cm-DBH were measured. Other factors including the size (diameter or height) differed between sites (Figs. 4 and S9) – only light and basal area related patterns where consistent. Panel *c* is the proportion of size groups at each site found in each light environment; the Tapajós displays higher mean one-hectare scale biomass growth.

model was significantly better than alternatives (i.e. model was separated from others by a ΔAIC greater than 2) and all factors were significant; the second best model included light transmittance and light absorption (ΔAIC = 4.12) and the third best model included just light transmittance (ΔAIC = 7.05). We extended the best model from Ducke to predict the variation of size group biomass growth in Ducke and the Tapajós.

Aggregating predictions of this model within each of the two forests by averaging groups of the same tree sizes across plots (Fig. 4b), and for each one-hectare plot by summing all size group predictions for the plot (Fig. 4a), we are able to predict 90% of variation in growth between size groups (P-value < 0.0001; Resid. SE = 0.07; 27 d.f.), or 25% of the variation between plots (P-value < 0.01 level; Resid. SE = 0.62; 35 d.f.). When we restricted plot level analysis to a single site, Ducke or the Tapajós, the LiDAR-based approach does not significantly predict variation (P-values 0.17 & 0.19 respectively).

The Shannon index of leaf area profiles predicted 27% of plot-to-plot variation in biomass growth (Fig. S10a in Appendix S1; growth = −6.675 + 2.800 × Shannon index; Resid. SE = 0.61; 35 d.f.; P-value < 0.001). In this case, the canopy Shannon index significantly captures plot level variation (favoured by 4.4 ΔAIC in comparison with a model including a site-factor alone). Plot-level growth predictions obtained from the size group model reported above were highly linearly related to the canopy Shannon index values (R^2 = 0.76; SE = 0.32, P-value < 0.0001, 35 d.f.). The canopy Shannon index was not related to plot-level variation in mortality, while it was the best predictor – 20% of variation – of net change in above-ground coarse wood biomass (net change = −30.805 + 9.203 × Shannon index; Resid. SE = 2.45; 35 d.f.; P-value < 0.01; Fig. S10b). Single-layer indices – LAI, light transmission to the understory, and total absorption – were, however, *not* able to predict plot growth (growth vs. LAI: R^2 = 0.01; P-value = 0.57, 35 d.f.).

Gap fraction and above-ground carbon dynamics

The demographic components of above-ground coarse wood carbon dynamics – biomass growth, loss to mortality and gain from recruitment to 10 cm-DBH – were significantly related to gap fraction in 1-ha plots (considering Tapajós and Ducke plots; Fig. 5 and Table S2 and 'Site Differences in Components of Above-ground Carbon Dynamics' in Appendix S1). Relationships were strongest when sampling over larger areas within sites, an analysis that allowed the inclusion of a third site, ZF2 (Table S2 in Appendix S1), giving R^2 values ranging from 0.31 to 0.67. Nonetheless, the combined effect of these components (net change in live above-ground biomass) was significantly related to gap fraction only at the one-hectare plot scale, where gap fraction explained a low proportion of variation in net change (13%). Offsetting trends of increasing biomass growth (gain) and mortality (loss) with gap fraction may explain why net biomass change does not covary as strongly with gap fraction as biomass growth. At the one-hectare plot scale, gap fraction predicted variation in biomass growth about as well as the Shannon index (27%).

DISCUSSION

We found that variation in canopy gap fraction, leaf area density and indices of light environments – estimated with airborne small-footprint LiDAR – predicted above-ground coarse wood production (biomass growth) from scales of one-hectare forest plots to sites ~500 km apart, predicting over a quarter of variation in small (1 ha) forest plots. At the landscape scale (10 ha) more relevant to

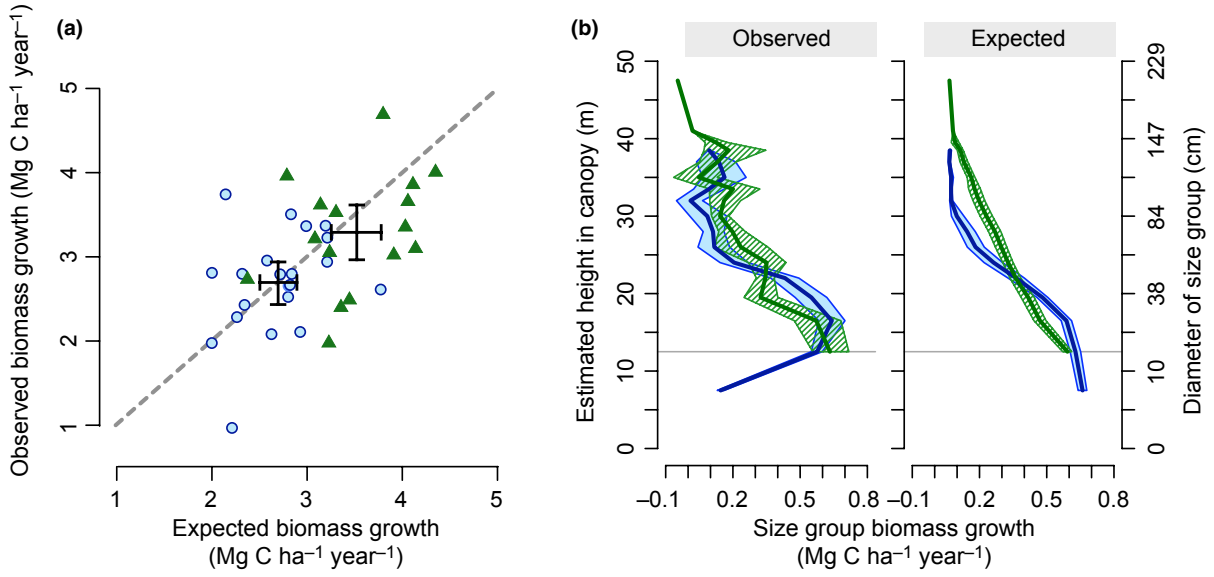

Figure 4 Panel *a* shows observed and expected biomass growth over one-hectare plots (N = 37), whereas panel *b* shows observed and expected size group biomass growth plotted vs. size group expected height and diameter on vertical axes. Sites are Ducke (*blue*, *solid* and *circles*) and Tapajós (*green*, *hashed* and *triangles*), while hashed (or solid) regions show resampling–estimated 95% confidence intervals (N=351). The statistical model – predicting size group biomass growth with LiDAR-estimated canopy variables (see Figs. 1 and 2) – was fit with Ducke data alone and then applied to both sites, predicting 25% of variation in biomass growth over one-hectare plots and 90% of the variation in the mean size-specific biomass growth. In panel *a*, whiskers are means and 95% CIs for sites based on plot scale variation.

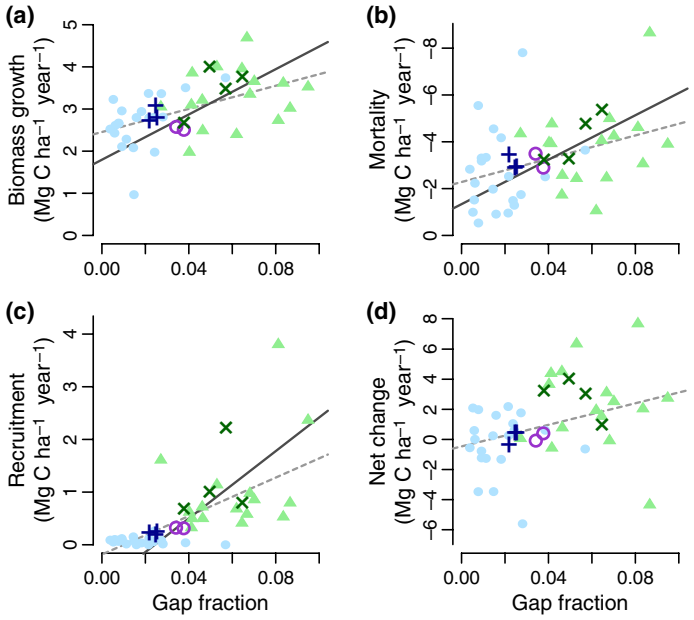

Figure 5 Demographic components of above-ground wood biomass dynamics in relation to canopy gap fraction for one-hectare plots ($N = 37$) and larger areas (sub-sites) within the Tapajós, Ducke and ZF2 sites ($N = 9$). Large symbols denote sub-sites in Ducke (*dark blue*, '+'), the Tapajós (*dark green*, '×') and ZF2 (*magenta*, 'O'), while the solid symbols are one-hectare scale plots of Ducke (*blue*, *circle*) and the Tapajós (*green*, *triangle*). Significant regressions are shown; solid lines are for sub-site data, whereas dashed lines are for plots (see Table S2 in Appendix S1 for statistics).

understanding the key question of large-scale carbon dynamics, R^2 values increased to over 50%. Vertical variation in canopy metrics appeared to be essential to biomass growth; metrics that were not sensitive to vertical structure such as average plot LAI were not related to variation in biomass growth. Gap fraction was a strong predictor of biomass growth and recruitment to 10-cm DBH, as well as biomass loss to mortality. Gap fraction, thus, appears to be a good metric of ecologically relevant canopy structural variation that influences biomass growth, while being mechanistically linked to biomass loss through tree mortality and gap formation.

Although estimates of leaf area density and the absorption of light incident to the canopy significantly predicted biomass growth, light availability was the strongest single predictor of variation in biomass growth and the only predictor that was consistently related to size group biomass growth at both sites (see Figs 3 and S9). Furthermore, this relationship was consistent in spite of significant differences in canopy structure and demographic history between sites: the Adolfo Ducke Reserve near Manaus (used to fit our height-structured model) has a low closed canopy with rapid light reduction in the upper-canopy relative to the carbon-accruing Tapajós National Forest ~500 km east in Pará (where we extended the model; Fig. 1). The consistency of this relationship suggests hypotheses to explain the role of canopy structure in above-ground carbon cycling, while providing a tool that in combination with LiDAR remote sensing may significantly increase understanding of the spatial heterogeneity of carbon dynamics in tropical forests.

The consistent relationship of size group biomass growth with mean light environment was the primary factor underlying significant plot and site level predictions. The proportions of variation explained by a model containing the light transmittance index alone were at minimum 89% of those explained by the full model for all scales of variation in biomass growth considered. This finding suggests, for example, that our ability to predict site differences in the division of biomass growth over forest size structure (see Fig. 4b) was due first to the consistency of biomass growth within light environments – detectable with LiDAR – and second to a difference in the distribution of light environments over size classes between the sites (see Fig. 3c). The factors that explain differences in canopy structure, therefore, predictably influence landscape carbon dynamics. It is crucial to determine the basis for this consistency to move from descriptive to mechanistic explanations for variation in above-ground carbon dynamics.

Our results supported the hypothesis (H1a) that leaves – or individual trees – optimise their productivity in the canopy to create consistent relationships between canopy light environments and biomass growth. In contrast, we did not find support for the alternative (H1b). Tapajós and Ducke experience different (1) rainfall and soil characteristics, (2) tree compositions and (3) disturbance histories (Vieira *et al.* 2004; Pyle *et al.* 2008). However, we do not have strong evidence to rule out the importance of such factors (H1b), particularly considering the substantial unexplained variation of components of carbon dynamics in one-hectare plots.

What optimisation process or processes would lead to consistent patterns of wood production in light environments? The optimisation mechanism at work appears to array leaf area and (or) leaf level productivity similarly over light environments in different plots and forest sites. The total leaf area associated with a size group is influenced by the recruitment, growth, and loss to mortality of trees and physiological factors, such as wood density and leaf allocation (Muller-Landau *et al.* 2006b; Coomes *et al.* 2012). Demographic processes are likely to respond dynamically to light environments and may, therefore, play roles in the optimisation mechanism (Kohyama 1993; Muller-Landau *et al.* 2006b). Although we found that size group wood production decreased in higher light (Fig. 3a), tree size distributions likely explain the declining pattern: larger size classes are associated with fewer individuals, less leaf area and therefore less growth. Future application of this method should focus on testing mechanisms explaining size structure.

Recent theories link the arrangement of leaf area in space with leaf level photosynthetic production and forest demographic processes (Moorcroft *et al.* 2001; Muller-Landau *et al.* 2006a; Strigul *et al.* 2008; West *et al.* 2009; Coomes *et al.* 2012). LiDAR is a natural source of data to compare and test these theories (Hurtt *et al.* 2004; Antonarakis *et al.* 2011), particularly if it can provide data on canopy environments across the forest size spectrum. The results of this study can be compared against key assumptions and predictions of theory. First, the metabolic theory of ecology predicts that wood production will converge on consistent distributions over stem diameter. We find, instead, evidence for a consistent distribution of biomass growth over light environments, and no relationship with stem diameter. The relative constancy of basal area specific biomass growth over light environments supports, however, the key 'energetic equivalence' assumption of metabolic theory that the average leaf area-specific productivity of each tree is equivalent. In this case, a similar distribution of light over individual leaves may be found across the size spectrum. Canopy optimisation of leaf angle and nitrogen content may help explain this pattern (Coomes *et al.* 2012;

Niinemets & Anten 2009). The packing of tree canopies and branches in space may also play a role (Coomes *et al.* 2012); the heterogeneity of leaf area over the vertical canopy profile in the Tapajós, however, may not be consistent with leaves filling space uniformly with 'perfect plasticity' (see Strigul *et al.* 2008).

Previously, airborne small footprint LiDAR has been largely limited to estimating standing above-ground biomass (e.g. Asner *et al.* 2010). Our results suggest that LiDAR data are rich, and can be used to make both theoretical and practical progress on problems related to tropical forest carbon dynamics. We show that by using LiDAR surveys of heterogeneity in canopy structure and associated light environments, we could map the components of the above-ground biomass dynamics that arise from tree demographic processes in mature tropical forests. An explicit size-structured model of canopy environments and two additional approaches – the canopy Shannon index and gap fraction – each succeeded in predicting 25% or more of the variation in biomass growth in one-hectare plots. Within mature forests, our results suggest that biomass growth can be estimated from LiDAR with much higher confidence as scale increases above one-hectare plots to the landscape scale. For example, resampling from the canopy Shannon index vs. biomass growth relationship to create hypothetical 50 ha forest plots, biomass growth was resolved to within 7% of the tree plot estimated value 95% of the time. This predictive skill is sufficient to help determine whether plots and sites are carbon sinks or sources to address debate about the carbon balance of tropical forests (see Gloor *et al.* 2009).

Given the potential for future climate change induced droughts that could drive tree mortality and alter canopy environments (Cox *et al.* 2004; Nepstad *et al.* 2007; Phillips *et al.* 2009), it is critically important to understand the canopy processes that regulate carbon dynamics. Although light has long been known to be important (Lambers *et al.* 2008; Niinemets & Anten 2009), the nature of the quantitative relationship between light and wood production across landscape scale variation in canopy structure has remained largely unknown. Using the novel datasets now derivable from LiDAR remote sensing we were able to reveal consistent relationships between wood growth and light environments over the forest size spectrum in sites with distinct climates and canopy structure. We expect future work to refine this approach and to rigorously test mechanistic theories of productivity and size-structured tree demography. Future airborne LiDAR surveys of larger areas across remote forest regions such as the Amazon will thus likely improve both theoretical understanding of the large-scale ecology of forest function, as well as empirical quantification of regional carbon budgets, necessary to inform policy decisions relevant to mitigation of anthropogenic climate change.

ACKNOWLEDGEMENTS

This work was supported by National Science Foundation awards (DDIG 0807221, DEB 0721140, OISE 0730305) and the National Air and Space Administration (contract NNX09AI33G) while Stark was also supported by an NSF GRFP and an NSF PIRE fellowship (also from OISE 0730305). Extensive scientific field and logistical support were provided by Brazilian institutions INPA-LBA, Embrapa Amazônia Oriental, INPA-Ecologia and PPBio (offices in Santarém and Manaus, Brazil). Risonaldo Lima Leal, Flávia Pezzini, Cleuton Pereira and a team of Santarém-area (Igarapé Branco Community) technicians provided extensive assistance in the field. We thank DA Coomes, three anonymous referees, BJ Enquist and ML Friesen for comments improving this article.

AUTHOR CONTRIBUTIONS

SCS designed the research, collected data, conducted analysis and wrote the manuscript. VL and JLW assisted with analysis and design. SRS contributed to research design, to airborne LiDAR data acquisition, to data analysis, and to writing. MOH, SMM, GGP and MAL contributed essential analytical tools and assisted in their implementation. GGP, MK and FRCC contributed important manuscript revisions. CVC and MTS managed primary field and LiDAR data set collections respectively, whereas VL, LFA, JS, YES, DOB, TKW, NH, PBC and RCO collected data and contributed to pre-analysis processing and investigation implementation.

REFERENCES

Antonarakis, A., Saatchi, S., Chazdon, R. & Moorcroft, P. (2011). Using lidar and radar measurements to constrain predictions of forest ecosystem structure and function. *Ecol. Appl.*, 21, 1120–1137.

Asner, G., Powell, G., Mascaro, J., Knapp, D., Clark, J., Jacobson, J. *et al.* (2010). High-resolution forest carbon stocks and emissions in the Amazon. *Proc. Natl. Acad. Sci. USA*, 107, 16738.

Brokaw, N. (1985). Gap-phase regeneration in a tropical forest. *Ecology*, 66, 682–687.

Castilho, C., Magnusson, W., de Araújo, R., Luizão, R., Luizão, F., Lima, A. *et al.* (2006). Variation in aboveground tree live biomass in a central Amazonian forest: effects of soil and topography. *Forest Ecol. Manag.*, 234, 85–96.

Cavaleri, M., Oberbauer, S., Clark, D., Clark, D. & Ryan, M. (2010). Height is more important than light in determining leaf morphology in a tropical forest. *Ecology*, 91, 1730–1739.

Chambers, J., Asner, G., Morton, D., Anderson, L., Saatchi, S., Espı´rito-Santo, F. et al. (2007). Regional ecosystem structure and function: ecological insights from remote sensing of tropical forests. *Trends Ecol. Evol.*, 22, 414–423.

Chave, J., Condit, R., Aguilar, S., Hernandez, A., Lao, S. & Perez, R. (2004). Error propagation and scaling for tropical forest biomass estimates. *Philos. Trans. R. Soc. Lond. Biol. Sci.*, 359, 409–420.

Chave, J., Andalo, C., Brown, S., Cairns, M., Chambers, J., Eamus, D. *et al.* (2005). Tree allometry and improved estimation of carbon stocks and balance in tropical forests. *Oecologia*, 145, 87–99.

Chave, J., Coomes, D., Jansen, S., Lewis, S., Swenson, N. & Zanne, A. (2009). Towards a worldwide wood economics spectrum. *Ecol. Lett.*, 12, 351–366.

Chen, Q., Gong, P., Baldocchi, D. & Xie, G. (2007). Filtering airborne laser scanning data with morphological methods. *Photogramm. Eng. Rem. S.*, 73, 175.

Clark, D., Olivas, P., Oberbauer, S., Clark, D. & Ryan, M. (2008). First direct landscape-scale measurement of tropical rain forest leaf area index, a key driver of global primary productivity. *Ecol. Lett.*, 11, 163–172.

Coomes, D., Holdaway, R., Kobe, R., Lines, E. & Allen, R. (2012). A general integrative framework for modelling woody biomass production and carbon sequestration rates in forests. *J. Ecol.*, 100, 42–64.

Cox, P., Betts, R., Collins, M., Harris, P., Huntingford, C. & Jones, C. (2004). Amazonian forest dieback under climate-carbon cycle projections for the 21st century. *Theor. Appl. Climatol.*, 78, 137–156.

Davis, T. & Richards, P. (1933). The vegetation of Moraballi Creek, British Guiana: an ecological study of a limited area of tropical rain forest. part i. *J. Ecol.*, 21, 350–384.

Enquist, B. & Niklas, K. (2002). Global allocation rules for patterns of biomass partitioning in seed plants. *Science*, 295, 1517–1520.

Feldpausch, T., Banin, L., Phillips, O., Baker, T., Lewis, S., Quesada, C. *et al.* (2010). Height-diameter allometry of tropical forest trees. *Biogeosciences*, 7, 7727–7793.

Feldpausch, T., Lloyd, J., Lewis, S., Brienen, R., Gloor, E., Monteagudo Mendoza, A. *et al.* (2012). Tree height integrated into pan-tropical forest biomass estimates. *Biogeosci. Disc.*, 9, 2567–2622.

Fownes, J. & Harrington, R. (1992). Allometry of woody biomass and leaf area in five tropical multipurpose trees. *J. Trop. For. Sci.*, 4, 317–330.

Gloor, M., Phillips, O., Lloyd, J., Lewis, S., Malhi, Y., Baker, T. *et al.* (2009). Does the disturbance hypothesis explain the biomass increase in basin-wide amazon forest plot data? *Glob. Change Biol.*, 15, 2418–2430.

Harding, D., Lefsky, M., Parker, G. & Blair, J. (2001). Laser altimeter canopy height profiles: methods and validation for closed-canopy, broadleaf forests. *Remote Sens. Environ.*, 76, 283–297.

Herault, B., Bachelot, B., Poorter, L., Rossi, V., Bongers, F., Chave, J. *et al.* (2011). Functional traits shape ontogenetic growth trajectories of rain forest tree species. *J. Ecol.*, 99, 1431–1440.

Hurtt, G., Dubayah, R., Drake, J., Moorcroft, P., Pacala, S., Blair, J. *et al.* (2004). Beyond potential vegetation: combining lidar data and a height-structured model for carbon studies. *Ecol. Appl.*, 14, 873–883.

Kohyama, T. (1993). Size-structured tree populations in gap-dynamic forest–the forest architecture hypothesis for the stable coexistence of species. *J. Ecol.*, 81, 131–143.

Lambers, H., Chapin, F. & Pons, T. (2008). *Plant Physiological Ecology*. 2nd edn. Springer, New York.

Lee, H., Slatton, K., Roth, B. & Cropper, W. (2009). Prediction of forest canopy light interception using three-dimensional airborne LiDAR data. *Int. J. Remote Sens.*, 30, 189–207.

Lewis, S., Phillips, O., Baker, T., Lloyd, J., Malhi, Y., Almeida, S., Higuchi, N. *et al.* (2004). Concerted changes in tropical forest structure and dynamics: evidence from 50 South American long-term plots. *Philos. Trans. B*, 359, 421.

MacArthur, R. & Horn, H. (1969). Foliage profile by vertical measurements. *Ecology*, 50, 802–804.

Malhi, Y., Roberts, J., Betts, R., Killeen, T., Li, W. & Nobre, C. (2008). Climate change, deforestation, and the fate of the Amazon. *Science*, 319, 169.

McWilliam, A., Roberts, J., Cabral, O., Leitao, M., de Costa, A., Maitelli, G. *et al.* (1993). Leaf area index and above-ground biomass of terra firme rain forest and adjacent clearings in Amazonia. *Funct. Ecol.*, 7, 310–317.

Moorcroft, P. (2006). How close are we to a predictive science of the biosphere? *Trends Ecol. Evol.*, 21, 400–407.

Moorcroft, P., Hurtt, G. & Pacala, S. (2001). A method for scaling vegetation dynamics: the ecosystem demography model (ED). *Ecol. Monogr.*, 71, 557–586.

Muller-Landau, H., Condit, R., Chave, J., Thomas, S., Bohlman, S., Bunyavejchewin, S. *et al.* (2006a). Testing metabolic ecology theory for allometric scaling of tree size, growth and mortality in tropical forests. *Ecol. Lett.*, 9, 575–588.

Muller-Landau, H., Condit, R., Harms, K., Marks, C., Thomas, S., Bunyavejchewin, S. *et al.* (2006b). Comparing tropical forest tree size distributions with the predictions of metabolic ecology and equilibrium models. *Ecol. Lett.*, 9, 589–602.

Nepstad, D., Tohver, I., Ray, D., Moutinho, P. & Cardinot, G. (2007). Mortality of large trees and lianas following experimental drought in an Amazon forest. *Ecology*, 88, 2259–2269.

Niinemets, Ü. & Anten, N. (2009). Packing the photosynthetic machinery: from leaf to canopy. In: *Photosynthesis in Silico: Understanding Complexity from Molecules to Ecosystems* (eds Laisk, A., Nedbal, L. & Govindjee). Springer, Dordrecht, The Netherlands, pp. 363–399.

Parker, G., Harding, D. & Berger, M. (2004). A portable LIDAR system for rapid determination of forest canopy structure. *Ecology*, 41, 755–767.

Parker, G., Lefsky, M. & Harding, D. (2001). Light transmittance in forest canopies determined using airborne laser altimetry and in-canopy quantum measurements. *Remote Sens. Environ.*, 76, 298–309.

Phillips, O., Aragão, L., Lewis, S., Fisher, J., Lloyd, J., López-González, G. *et al.* (2009). Drought sensitivity of the Amazon rainforest. *Science*, 323, 1344.

de Pury, D. & Farquhar, G. (1997). Simple scaling of photosynthesis from leaves to canopies without the errors of big-leaf models. *Plant Cell Environ.*, 20, 537–557.

Pyle, E., Santoni, G., Nascimento, H., Hutyra, L., Vieira, S., Curran, D. *et al.* (2008). Dynamics of carbon, biomass, and structure in two Amazonian forests. *J. Geophys. Res*, 113, G00B08. DOI: 10.1029/2007JG000592.

Richardson, J., Moskal, L. & Kim, S. (2009). Modeling approaches to estimate effective leaf area index from aerial discrete-return LIDAR. *Agr. Forest Meteorol.*, 149, 1152–1160.

Saleska, S., Miller, S., Matross, D., Goulden, M., Wofsy, S., da Rocha, H. *et al.* (2003). Carbon in Amazon forests: unexpected seasonal fluxes and disturbance-induced losses. *Science*, 302, 1554.

Shinozaki, K., Yoda, K., Hozumi, K. & Kira, T. (1964). A quantitative analysis of plant form–the pipe model theory i. basic analyses. *Japan. J. Ecol.*, 14, 97–105.

da Silva, R., dos Santos, J., Tribuzy, E., Chambers, J., Nakamura, S. & Higuchi, N. (2002). Diameter increment and growth patterns for individual tree growing in Central Amazon, Brazil. *Forest Ecol. Manag.*, 166, 295–301.

Sitch, S., Huntingford, C., Gedney, N., Levy, P., Lomas, M., Piao, S. *et al.* (2008). Evaluation of the terrestrial carbon cycle, future plant geography and climate-carbon cycle feedbacks using five Dynamic Global Vegetation Models (DGVMs). *Glob. Change Biol.*, 14, 2015–2039.

Strigul, N., Pristinski, D., Purves, D., Dushoff, J. & Pacala, S. (2008). Scaling from trees to forests: tractable macroscopic equations for forest dynamics. *Ecol. Monogr.*, 78, 523–545.

Tang, H., Dubayah, R., Swatantran, A., Hofton, M., Sheldon, S., Clark, D., et al. (2012). Retrieval of vertical lai profiles over tropical rain forests using waveform lidar at La Selva, Costa Rica. *Remote Sens. Environ.*, 124, 242–250.

Todd, K., Csillag, F. & Atkinson, P. (2003). Three-dimensional mapping of light transmittance and foliage distribution using lidar. *Can. J. Remote Sens.*, 29, 544–555.

Vieira, S., De Camargo, P., Selhorst, D., Da Silva, R., Hutyra, L., Chambers, J. *et al.* (2004). Forest structure and carbon dynamics in Amazonian tropical rain forests. *Oecologia*, 140, 468–479.

West, G., Enquist, B. & Brown, J. (2009). A general quantitative theory of forest structure and dynamics. *Proc. Natl. Acad. Sci. USA*, 106, 7040.

SUPPORTING INFORMATION

Additional Supporting Information may be downloaded via the online version of this article at Wiley Online Library (www.ecologyletters.com).

As a service to our authors and readers, this journal provides supporting information supplied by the authors. Such materials are peer-reviewed and may be re-organised for online delivery, but are not copy-edited or typeset. Technical support issues arising from supporting information (other than missing files) should be addressed to the authors.

Editor, Jerome Chave
Manuscript received 23 May 2012
First decision made 29 June 2012
Manuscript accepted 6 August 2012